Cooperative Localization and Control for Multi-Robot Manipulation

J. Spletzer, A. K. Das, R. Fierro, C. J. Taylor, V. Kumar, and J. P. Ostrowski

GRASP Laboratory – University of Pennsylvania
Philadelphia, PA, 19104, USA

{spletzer, aveek, rfierro, cjtaylor, kumar, jpo}@grasp.cis.upenn.edu

Abstract

We describe a framework for coordinating multiple robots in cooperative manipulation tasks in which vision is used for establishing relative position and orientation and maintaining formation. The two key contributions are a cooperative scheme for localizing the robots based on visual imagery that is more robust than decentralized localization, and a set of control algorithms that allow the robots to maintain a prescribed formation (shape and size). The ability to maintain a prescribed formation allows the robots to "trap" objects in their midst, and to "flow" the formation to a desired position. We derive the cooperative localization and control algorithms and present experimental results that illustrate the implementation and the performance of these algorithms.

Figure 1: The Clodbuster^{TM} team used for experiments.

1 Introduction

It has long been recognized that there are several tasks that can be performed more efficiently and robustly using multiple robots [1]. We are motivated by applications in which robots can be coordinated to develop three-dimensional maps of unknown or partially known environments [2, 3], and tasks where robots can cooperate to manipulate and transport objects without using special purpose effectors or material handling accessories [4]. Our main focus in this paper is on cooperative manipulation. We refer the reader to [5] to our previous work on cooperative localization and mapping.

We consider an environment where there is no access to any global positioning system and the main sensing modality is vision. We allow the robots to communicate, but we would like the performance of the system to degrade gracefully in the absence of a communication network. Our ultimate goal is to be able to organize and coordinate a group of robots to approach, grasp and manipulate a specified object from a prescribed location to a final destination.

In grasping and manipulation tasks, form and force closure properties and grasp stability lead to important constraints in manipulation [6, 7]. Usually these constraints are a strong function of the specific manipulator(s) or effector(s) and the control algorithms used
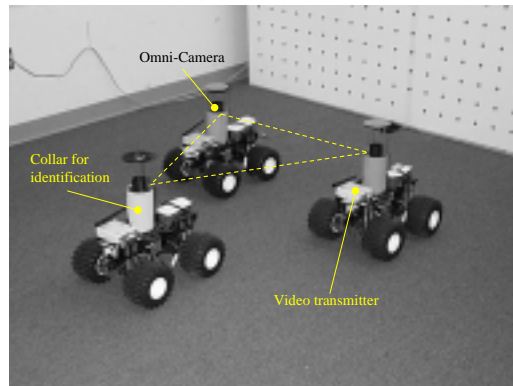
to control the manipulator(s). Our goal is to pursue a fixture-less approach to manipulation where the mobile robots are not equipped with any special purpose arm or gripper.

There is a significant body of literature in which the quasi-static assumption is used effectively to develop a paradigm for multi-robot manipulation [8, 9, 10]. In this paradigm, the robots can cooperatively push an object, generally maintaining a specified orientation to a goal position. In such situations, it is necessary to monitor the position and orientation of the manipulated object and to ensure that the perturbations caused by pushing are relatively small so that dynamics can be safely ignored.

In contrast, we propose a paradigm in which the manipulated object can be trapped or caged by a group of robots in formation, and the control of the flow of the group allows the transportation or manipulation of the grasped object. In this paradigm, the dynamics of the object and the robot-object interactions are never modeled, as is the case in [4]. Instead, by guaranteeing the shape of the formation, we can keep the manipulated object trapped amidst the robots. This approach can be potentially scaled to multiple (tens and hundreds) robots and to higher speeds of operation. In contrast to other approaches to caging [11, 12], we do not require conditions for form closure to be maintained. Neither do we need to

plan the manipulation task as in [13]. Given the shape of the object, we can use well-known algorithms for planning form-closed grasps [14] to derive the shape of the formation, and the allowable tolerance on shape changes.

The two key contributions in this paper are (1) a cooperative scheme for localizing the robots based on visual imagery that is more robust than decentralized localization; and (2) a set of control algorithms that allow the robots to maintain a prescribed formation (shape and size). The ability to maintain a prescribed formation allows the robots to "trap" objects in their midst and to "flow" the formation to a desired point guaranteeing that the object is transported to that point.

Our localization approach builds on work by Kurazume *et al.*. They proposed using members of a robot team as mobile landmarks for position estimation, and implemented this as a more accurate and robust alternative to robot positioning via dead reckoning [15]. The procedure was termed *Cooperative Positioning* (CP). One method - Type II positioning - allowed the relative position of the team to be recovered up to a scale factor solely by sharing relative azimuth and elevation angle measurements. We propose an extension to this positioning method whereby both the relative position *and* orientation of the platforms can be recovered solely from angular measurements gleaned from the imagery. The robot team used to demonstrate this localization method can be seen in Figure 1. On-board omnidirectional video cameras provide us with a passive means for obtaining all of the necessary angle information with a single sensor. Since this localization method is extendible to n robots with resulting improvements in performance, it offers significant potential benefits to multi-robot applications.

Incorporating this technique, we next describe a framework for cooperative localization and control of robot formations that can be used for distributed manipulation of objects. Specifically, we consider a team of three non-holonomic mobile robots that are required to follow a prescribed trajectory while maintaining a desired formation. A robot designated as the *reference* robot follows a trajectory generated by a high-level planner. Depending on the task at hand *i.e.*, holding or constraining, we can choose among controllers which track different output variables (as described in Section 3). The individual controllers themselves can be decentralized as in [16], relying on velocity estimation of team members. In the present work we have information sharing between three robots about their relative configurations in the formation by way of the cooperative localizer. This allows for a centralized controller that is potentially more robust to sensor noise and uncertainties related to actuator dynamics. In applications involving a large team of robots, we can decompose the team into smaller groups allowing our localizer and controller to be used for individual groups, with lim-

ited communication between the groups.

The rest of this paper is organized as follows. Section 2 presents the mathematical details and implementation of the cooperative localization proposed here. In Section 3 we present a set of controllers that requires reliable cooperative localization for formation control purposes. Experimental results illustrate our application of this methodology to the implementation of cooperative control of robot formations and distributed manipulation are in Section 4. Finally, some concluding remarks and future work ideas are given in Section 5.

2   Cooperative $3D$ Localization

Cooperative $3D$ localization can be accomplished with a team of three (or more) robots where each robot is capable of measuring the direction to the other members of the team. This information can be applied to team relative tasks such as cooperative manipulation as demonstrated in this paper, or extended to global pose tasks as shown in our previous work in cooperative mapping [17].

In our current implementation, direction measurements to other robots were obtained from the omnidirectional imagery acquired with the on-board catadioptric camera systems. One of the primary advantages of catadioptric cameras for this application is that they afford a single effective point of projection. This means that, after an appropriate calibration, every point in the omnidirectional image can be associated with a unique ray through the focal point of the camera.
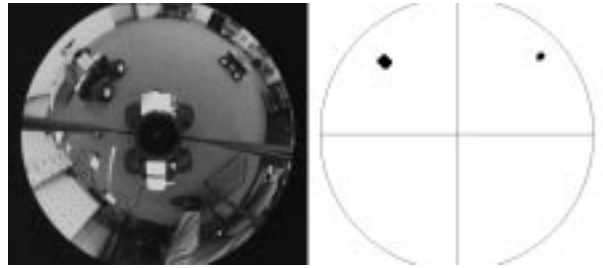

Figure 2: Actual and color segmented images. Direction vectors were estimated from the blob CGs.

To facilitate team member identification, we fitted each of the robots with a colored cylindrical collar. This yielded a $360°$ symmetrical target about each robot's optical axis. We then used a color extractor operating in YUV space to isolate these targets in each robot's image. The color extractor takes advantage of YU and YV *look-up tables* to significantly reduce processing time, and is capable of segmenting up to 8 colors simultaneously. By applying a blob extractor to the subsequent image, we obtained the center of gravity (CG) of the collar which was used to estimate the required direction vectors. A sample

omnidirectional image and the corresponding segmented image are shown in Figure 2. As implemented, the localizer runs at 14-15 Hz with all three robots operating from a single PC.

In Figure 3 the unit vectors $\hat{u}_{ij} \in \mathbb{R}^3$ denote the direction between robot i and robot j expressed in the coordinate frame of robot i. Let $^iT_j \in \mathbb{R}^3$ and $^iR_j \in SO(3)$ represent respectively the translation and rotation of robot j with respect to the frame of reference of robot i. These vectors are derived from the images using the procedure described in the previous paragraphs. Without loss of generality we can choose the reference frame of robot 1 as our base frame of reference and recover the configuration of the robot team by recovering the positions and orientations of the other robots with respect to this frame.
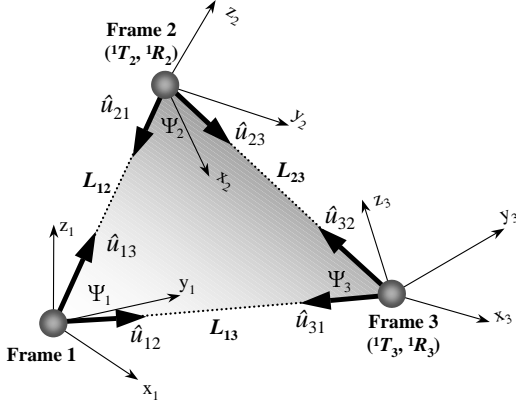

Figure 3: Three-dimensional geometry for agent localization.

In each frame, the internal angle between the direction vectors to the other two robots (ψ_i) can be determined from their scalar product; for instance $\psi_2 = \cos^{-1}(\hat{u}_{21} \cdot \hat{u}_{23})$. With this angle information, the translation between the frames can readily be determined to a scale factor by applying the sine rule to the shaded triangle in Figure 3. Arbitrarily setting the length of L_{23} in this figure to 1 (our chosen scale), we obtain the relative position for each of the agents as:

$$^1T_2 \quad = \quad L_{12}\hat{u}_{12} = \frac{\sin(\cos^{-1}(\hat{u}_{21} \cdot \hat{u}_{23}))}{\sin(\cos^{-1}(\hat{u}_{13} \cdot \hat{u}_{12}))} \hat{u}_{12} \quad (1)$$

$$^1T_3 \quad = \quad L_{13}\hat{u}_{13} = \frac{\sin(\cos^{-1}(\hat{u}_{32} \cdot \hat{u}_{31}))}{\sin(\cos^{-1}(\hat{u}_{13} \cdot \hat{u}_{12}))} \hat{u}_{13} \quad (2)$$

Position vectors relative to other frames can also be obtained by using the corresponding unit vectors. With the position of agents known, we only require the relative orientations of the frames to complete the localization procedure. To accomplish this, we note that the vectors ^jT_i and ^iT_j should have equal magnitude, but opposite direction when related by the corresponding rotation matrix

^jR_i. We note a similar relationship between the vectors $^jTi - ^jTk$ and ^iT_k. From these, we obtain the following pairs of equations.

$$-^1T_2 = {}^1R_2{}^2T_1, \qquad ^1T_3 - {}^1T_2 = {}^1R_2{}^2T_3$$
$$-^1T_3 = {}^1R_3{}^3T_1, \qquad ^1T_2 - {}^1T_3 = {}^1R_3{}^3T_2 \quad (3)$$

With all translation vectors known to a scale factor, the problem of solving for each rotation matrix reduces to the form:

$$\boldsymbol{R}a_i = b_i \qquad i \in [1,2] \quad (4)$$

This can be rephrased as the following optimization problem:

$$\min_R \sum_i \left\| \boldsymbol{R}a_i - b_i \right\|^2 \quad (5)$$

The rotation matrix which minimizes this expression can be computed in closed form as follows:

$$\boldsymbol{R} = (M^T M)^{-1/2} M^T \quad (6)$$

where $M = \sum_i a_i b_i^T$ [18].

Again recall that this solution yields the pose of the team *to a scale factor*. In order to obtain metric results, a means to recover the scale is necessary. This can be accomplished if the length of any one of the translation vectors between frames can be determined. In our experiments the robots were constrained to move on a flat surface. Since the geometry of each robot was known, any robot could gauge the distance to its teammates based on the radial distance to the extracted blobs in the image. The smaller the range, the closer the blob will appear to the image center. As a result, we have a means by which each robot can provide two estimates of the scale. We use the redundant estimates from all three to obtain the overall scale factor and the relative pose of the team. The accuracy of this implementation is discussed in Section 4.

This solution offers an improvement over methods presented previously, in that we obtain the relative position and orientation of the robot team solely from angular measurements without requiring that the angular estimates be referenced to a common axis like the gravity vector. This eliminates the need for the additional sensors that were required to measure agent orientation in previous implementations [15]. This localization method is readily extendible to n robots with resulting improvements in performance. It is also more robust than the completely decentralized localizer used in our previous work [23], where an extended Kalman filter is used to estimate each neighboring robots position and orientation using a kinematic model of the robot.

3 Formation Control

3.1 Modeling

In this section, we consider a group of 3 nonholonomic mobile robots and describe controllers that use the cooperative localization scheme derived previously. First, we will assume that the robots are planar and have two independent inputs. This means we have to restrict the robot control laws to those that regulate two outputs. Second, we assume that the robots are assigned labels from 1 through 3 which restrict the choice of control laws. Robot 1 (denoted R_1 here) is the leader of the group and follows a trajectory generated by a high-level planner $g(t) \in SE(2)$. We adopt a simple kinematic model for the nonholonomic robots. The kinematics of the ith–robot are given by

$$\dot{x}_i = v_i \cos\theta_i, \quad \dot{y}_i = v_i \sin\theta_i, \quad \dot{\theta} = \omega_i \quad (7)$$

where $\boldsymbol{x}_i \equiv (x_i, y_i, \theta_i) \in SE(2)$, and v_i and ω_i are the linear and angular velocities, respectively. Most commercially available robots do not allow the direct control of forces or torques. Instead they incorporate motor controllers that allow the specification of v_i and ω_i. Thus we will treat these as our inputs.

In Figure 4, we show the geometry of a three-robot configuration. To maintain relative distances and orientations, we present two controllers adopted from [19, 17] and derive a third controller which is motivated by the superior cooperative localizer discussed in Section 2.
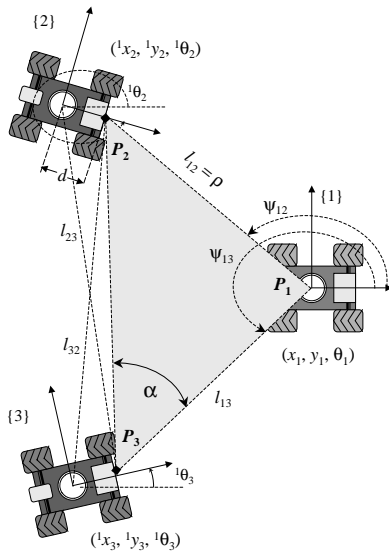

Figure 4: 3-Robot Formation Control Geometry.

3.2 Separation–Bearing Control

By using this controller, robot R_2 follows R_1 with a desired separation l_{12}^d and desired relative bearing ψ_{12}^d. Similarly, R_3 follows R_1 with a desired separation l_{13}^d

and desired relative bearing ψ_{13}^d. The control velocities for the *follower* robots are computed using I/O feedback linearization. In [16] we have shown that, under certain reasonable assumptions on the leader's trajectory, the internal dynamics of the follower are stable and its output converges exponentially to the desired values.

Since there is no interaction/communication between the followers R_2 and R_3, collisions (*i.e.*, $l_{23} \approx 0$ in Figure 4) may occur for some initial conditions or leader's trajectories. It is important to realize that stability of each agent in formation is a necessary but not a sufficient condition for successfully accomplishing a formation task. However, this limitation can be overcome by directly controlling the separation between R_2 and R_3.

In [16], this was accomplished through the separation–separation controller which allows R_3 to follow R_1 and R_2 with desired separations l_{13}^d and l_{23}^d, respectively. If the leader's trajectory is well-behaved, then the three-robot formation system can be shown to be stable and no collisions will occur.

3.3 Dilation Control

This controller allows robot R_2 to maintain a desired separation ρ^d and desired bearing ψ_{12}^d respect to R_1, see Figure 4. R_3 follows R_1 and R_2 with desired relative bearings ψ_{13}^d and ψ_{23}^d, respectively. By changing the *dilation* factor, ρ, the formation can be contracted or expanded in size while preserving the shape. In this case, the kinematic equations become

$$\dot{\boldsymbol{z}}_3 = \boldsymbol{A}_3\boldsymbol{u}_3 + \boldsymbol{b}_3, \quad \dot{\theta}_2 = \omega_2, \quad \dot{\theta}_3 = \omega_3 \quad (8)$$

where $\boldsymbol{z}_3 = \begin{bmatrix} \rho & \psi_{12} & \psi_{13} & \psi_{23} \end{bmatrix}^T$ is the system output, $\boldsymbol{u}_3 = \begin{bmatrix} v_2 & \omega_2 & v_3 & \omega_3 \end{bmatrix}^T$ is the input vector, and

$$\boldsymbol{A}_3 = \begin{pmatrix} \cos\gamma_{12} & d\sin\gamma_{12} & 0 & 0 \\ \frac{-\sin\gamma_{12}}{l_{12}} & \frac{d\cos\gamma_{12}}{l_{12}} & 0 & 0 \\ 0 & 0 & \frac{-\sin\gamma_{13}}{l_{13}} & \frac{d\cos\gamma_{13}}{l_{13}} \\ \frac{\sin\psi_{23}}{l_{23}} & -1 & \frac{-\sin\gamma_{23}}{l_{23}} & \frac{d\cos\gamma_{23}}{l_{23}} \end{pmatrix}$$

$$\boldsymbol{b}_3 = \begin{pmatrix} -v_1\cos\psi_{12} \\ \frac{v_1\sin\psi_{12}}{l_{12}} - \omega_1 \\ \frac{v_1\sin\psi_{13}}{l_{13}} - \omega_1 \\ 0 \end{pmatrix}$$

$$\gamma_{ij} = \theta_i + \psi_{ij} - \theta_j$$

By applying I/O feedback linearization, the control velocities for the *follower* robots are given by

$$\boldsymbol{u}_3 = \boldsymbol{A}_3^{-1}(\boldsymbol{p}_3 - \boldsymbol{b}_3) \quad (9)$$

where $\boldsymbol{p}_3$ is an auxiliary control input given by

$$\boldsymbol{p}_3 = \begin{pmatrix} k_1(l_{12}^d - l_{12}) \\ k_2(\psi_{12}^d - \psi_{12}) \\ k_2(\psi_{13}^d - \psi_{13}) \\ k_2(\psi_{23}^d - \psi_{23}) \end{pmatrix}$$

k_1, $k_2 > 0$ are design controller gains. The linearized closed-loop system becomes

$$\dot{z}_3 = p_3, \quad \dot{\theta}_2 = \omega_2, \quad \dot{\theta}_3 = \omega_3 \qquad (10)$$

In the following, we prove that the closed-loop system is stable. Since we are using I/O feedback linearization [20], the output vector z_3 will converge to the desired value z_3^d arbitrarily fast. However, a complete stability analysis requires the study of the internal dynamics of the robots *i.e.*, the heading angles θ_2 and θ_3 which depend on the controlled angular velocities ω_2 and ω_3, respectively.

Theorem 3.1 *Assume that the lead vehicle's linear velocity along the path $g(t) \in SE(2)$ is lower bounded i.e., $v_1 \geq V_{\min} > 0$, its angular velocity is also bounded i.e., $\|\omega_i\| < W_{\max}$, the relative velocity $\delta_v \equiv v_1 - v_2$, relative angular velocity $\delta_\omega \equiv \omega_1 - \omega_2$, and relative orientation $\delta_\theta \equiv \theta_1 - \theta_2$ are bounded by small positive numbers ε_1, ε_2, ε_3, and the initial relative orientation $\|\theta_1(t_0) - \theta_j(t_0)\| < c_j \pi$ with $0 < c_j < 1$ and $j = 1, 2$. If the control input (9) is applied to $R_{2,3}$, then the formation is stable and the system output z_3 in (10) converges exponentially to the desired value z_3^d.*

Proof: Let the system error $e = [e_1 \cdots e_6]^T$ be defined as

$$e_1 = \rho^d - \rho, \quad e_2 = \psi_{12}^d - \psi_{12}, \quad e_3 = \theta_1 - \theta_2$$
$$e_4 = \psi_{13}^d - \psi_{13}, \quad e_5 = \psi_{23}^d - \psi_{23}, \quad e_6 = \theta_1 - \theta_3 \quad (11)$$

First we need to show that the internal dynamics of R_2 are stable *i.e.*, the orientation error e_3 is bounded. Thus, we have

$$\dot{e}_3 = \omega_1 - \omega_2$$

after some algebraic simplification, we obtain

$$\dot{e}_3 = -\frac{v_1}{d} \sin e_3 + \eta_1(e_3, \omega_1, e_1, e_2) \qquad (12)$$

where

$$\eta_1(t, e_3) = (1 - \frac{\rho}{d}\cos(e_3 + \psi_{12}))\omega_1$$
$$- \frac{1}{d}(k_1 e_1 \sin(e_3 + \psi_{12}) + k_2 e_2 \rho \cos(e_3 + \psi_{12}))$$

The nominal system *i.e.*, $\eta_1(t, e_3) = 0$ is given by

$$\dot{e}_3 = -\frac{v_1}{d}\sin e_3 \qquad (13)$$

which is (locally) exponentially stable provided that the velocity of the lead robot $v_1 > 0$ and $\|e_3\| < \pi$. Since ω_1 is bounded, it can be shown that $\|\eta_1(t, e_3)\| \leq \delta_1$. By using stability theory of perturbed systems [21], and using theorem's condition $\|e_3(t_0)\| < c_1\pi$, then

$$\|e_3(t)\| \leq \sigma_1, \qquad \forall\, t \geq t_1$$

for some finite time t_1.

Now for R_3, we follow the same procedure. However, in this case we require the conditions on relative velocities and orientations of R_1 and R_2.

$$\dot{e}_6 = \omega_1 - \omega_3$$

after some work, we have

$$\dot{e}_6 = -\frac{v_1}{d}\sin e_6 + \eta_2(e_6, \omega_1, e_4, e_5, \delta_v, \delta_\theta, \delta_\omega) \quad (14)$$

where the nominal system *i.e.*, $\eta_2(t, e_6) = 0$ is (locally) exponentially stable provided that the velocity of the lead robot $v_1 > 0$ and $\|e_6\| < \pi$. Since $\|\omega_i\| < W_{\max}$, $\|\delta_v\| < \varepsilon_1$, $\|\delta_\omega\| < \varepsilon_2$ and $\|\delta_\theta\| < \varepsilon_3$, it can be shown that $\|\eta_2(t, e_6)\| \leq \delta_2$. Knowing that $\|e_6(t_0)\| < c_2\pi$ for some positive constant $c_2 < 1$, then

$$\|e_6(t)\| \leq \sigma_2, \qquad \forall\, t \geq t_2$$

for some finite time t_2.

$\square$

Remarks By controlling ρ and, for instance the angle α the formation shape can be easily expanded or contracted. This behavior is useful in cooperative localization and mapping where the scale factor of the formation triangle needs to be fixed. Moreover, the control objective could be maintaining the angle α in Figure 4 constant. Thus the formation shape can change its size based on environmental conditions *e.g.*, obstacles, narrow corridors, and so forth.

In the next section, we present experimental results using a group of car-like vehicles equipped with omnidirectional vision sensor. We illustrate our cooperative control framework in applications ranging from formation keeping to manipulation tasks.

4 Experimental Results
4.1 The Platform

The cooperative localizer was implemented on the GRASP Lab's Clodbuster^{TM} (CB) robots. The CB platform is based on the Tamiya Clodbuster^{TM} radio controlled truck. Each CB is equipped with an omnidirectional camera as its sole sensor [22]. This yields a $360°$ field of view (FOV) of the environment, and allows each agent to maintain visual contact with all other team members simultaneously. The platform lacks on-board processing. As a result, video data from all three agents are sent to a single remote computer for processing via a wireless 2.4 GHz video transmitter. Velocity and heading control signals are sent from the command computer to the vehicles as necessary. This reduces the cost and size of the platform, and makes it simple to coordinate the data processing and control operations. The CB team used for localization and formation control experiments can be seen in Figure 1.

4.2 Formation Control

Initial experiments in formation control were intended to validate the dynamic localization implementation and corresponding control approach. As a result, the first phase of experiments examined stable formations following trajectories of straight lines or gradual arcs. Video data from these trials were recorded using a calibrated overhead camera. This allowed "ground truth" position data of the formation to be recorded and analyzed off-line along with the localizer position estimates. Results from a representative trial can be found in Figures 5 and 6.
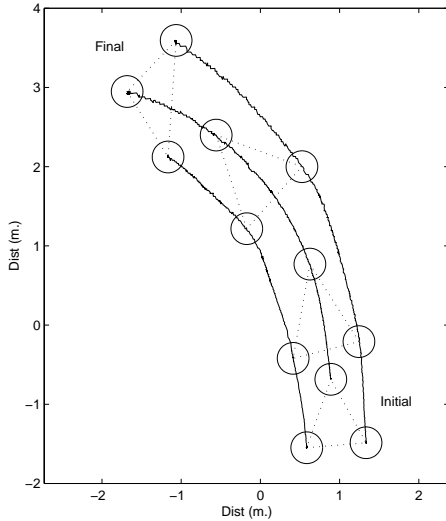

Figure 5: Simple Trajectory for a Triangular Formation

In this trial, the desired formation was an isosceles triangle where both followers maintained a distance of 1.0 m from the leader, and a separation of 0.7 m. Figure 5 shows the actual formation trajectory on the ground plane. Figure 6 contrasts the measured leader-follower separation distances with those calculated by the localizer. Results are for the most part satisfactory, with mean separation differences of 3.2% and 5.5% for the left and right side followers, respectively. Discontinuities in localizer data are due to corrupted image data resulting from the remote video transmission. Typical image corruption rates were 15-20% for each robot, leaving periods of time where no localization was possible.

The actual separation is always greater than the desired separation during motion because we use a pure feedback controller. It is possible to incorporate a feedfoward component either by prescribing a plan to all the robots, or by allowing the followers to estimate the leader's velocity. Our preliminary experiments with an Extended Kalman Filter for velocity estimation [16, 17] show improved performance. We are currently in the process of integrating nonlinear feed-forward controllers using velocity estima-
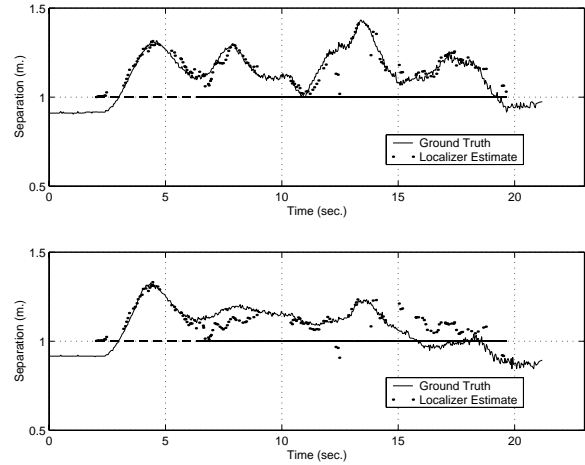

Figure 6: Follower Separation Distances: Actual & Localization Estimates

tion [23] to obtain better error tracking performance.

Following this concept validation, additional formations were examined to investigate the robustness of the proposed framework. These included different formation orientations, separation distances, etc. Results remained consistent with those obtained in earlier runs, as demonstrated in Figure 7 where followers maintained relative pose to the leader driving in a circular trajectory. Data points missing in the left side of the figure were outside the overhead camera's field of view.
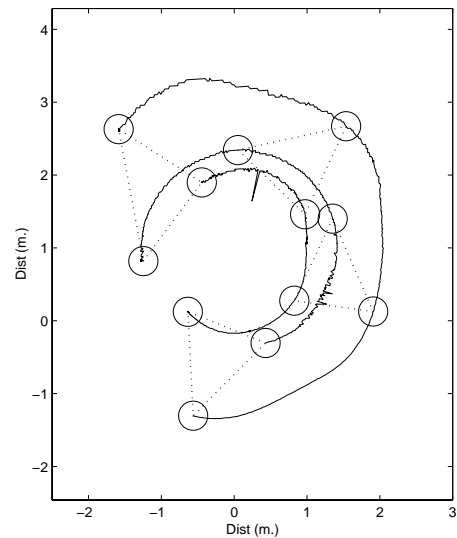

Figure 7: Circular Trajectory for a Triangular Formation

4.3 Cooperative Manipulation

The ability to maintain a prescribed formation allows the robots to "trap" objects in their midst and to "flow" the formation - guaranteeing that the object is transported

to the desired position.

With the ability to cooperatively localize and maintain formation, we proceeded to apply these two enabling technologies to a manipulation application. Two sets of experiments were conducted using a box as the object to be manipulated. In both cases the initial team configuration was a triangular formation centered around the box, and the goal was to flow the now encumbered formation along a trajectory generated by the leader. However, the trials differed with respect to formation. During the first set of trials, the formation was relaxed - allowing a separation between the box front and the lead robot. A constraining formation was used for the second example, where the box was in contact with all three robots during the formation flow. Several images from a sample run of the latter case are in Figure 8.

Figure 8: Distributed Manipulation Demonstration

Despite this control strategy not accounting for changes in the object's pose, the formation was typically successful in its manipulation task over the tested trajectories. As expected, the constrained case allowed for less lateral object motion with respect to the formation flow.

These experiments, while not an exhaustive investigation of cooperative manipulation, demonstrate the potential for cooperative vision based localization and formation control. As a next step, we are currently working on integrating object recognition and algorithms for choosing appropriate formations for a given object shape.

Acknowledgements

5   Conclusions

In this paper we presented a paradigm for cooperative manipulation in which the manipulated object can be trapped or caged by a group of robots in formation, and the control of the flow of the group allows the transportation or manipulation of the grasped object. To demonstrate this, two enabling technologies were derived and implemented. These were (1) a cooperative scheme for localizing the robots based on visual imagery that is more robust than decentralized localization; and (2) a set of control algorithms that allow the robots to maintain a prescribed formation (shape and size). In this paradigm, it is not necessary to model the dynamics of the object and the robot-object interactions. This allows the approach to be potentially scaled to multiple (tens and hundreds) robots and to higher speeds of operation. Our current and future work addresses the use of visual information to determine object geometry and to choose formations, and to decompose a team of many robots into smaller groups for localization and control.

References

[1] L. E. Parker, "Current state of the art in distributed autonomous mobile robotics," in *Distributed Autonomous Robotic Systems*, L. E. Parker, G. Bekey, and J. Barhen, Eds., vol. 4, pp. 3–12. Springer, Tokio, 2000.

[2] C. J. Taylor, "Video plus," Feb 2000, IEEE Workshop on Omnidirectional Vision 2000.

[3] L. Iochhi, K. Konolige, and M. Bayracharya, "A framework and architecture for multi-robot coordination," in *Proc. ISER00, Seventh International Symposium on Experimental Robotics*, Honolulu, Hawaii, Dec. 2000.

[4] T. Sugar and V. Kumar, "Control and coordination of multiple mobile robots in manipulation and material handling tasks," in *Experimental Robotics VI: Lecture Notes in Control and Information Sciences*, P. Corke and J. Trevelyan, Eds., vol. 250, pp. 15–24. Springer-Verlag, 2000.

[5] C. J. Taylor, "Videoplus: A method for capturing the structure and appearance of immersive environment," *Second Workshop on 3D Structure from Multiple Images of Large-scale Environments*, 2000.

[6] W. S. Howard and V. Kumar, "On the stability of grasped objects," *IEEE Trans. Robot. Automat.*, vol. 12, no. 6, pp. 904–917, 1996.

[7] J. C. Trinkle, "On the stability and instantaneous velocity of grasped frictionless objects," *IEEE Trans. Robot. Automat.*, vol. 8, no. 5, 1992.

[8] L. Parker, "Alliance: An architecture for fault tolerant multi-robot cooperation," *IEEE Trans. Robot. Automat.*, vol. 14, pp. 220–240, April 1998.

[9] M. Mataric, M. Nilsson, and K. Simsarian, "Cooperative multi-robot box pushing," in *IEEE/RSJ International Conf. on Intelligent Robots and Systems*, Pittsburgh, PA, Aug 1995, pp. 556–561.

[10] D. Rus, B. Donald, and J. Jennings, "Moving furniture with teams of autonomous robots," in *IEEE/RSJ International Conf. on Intelligent Robots and Systems*, Pittsburgh, PA, Aug 1995, pp. 235–242.

[11] E. Rimon and A. Blake, "Caging 2D bodies by one-parameter two-fingered gripping systems," in *IEEE International Conf. on Robotics and Automation*, Minneapolis, MN, Apr 1996, pp. 1458–1464.

[12] E. Rimon and J. W. Burdick, "Mobility of bodies in contact–i: A new 2nd order mobility index for multiple-finger grasps," *IEEE Trans. Robot. Automat.*, vol. 2, no. 4, pp. 541–558, 1998.

[13] A. Sudsang and J. Ponce, "A new approach to motion planning for disc-shaped robots manipulating a polygonal object in the plane," in *Proc. IEEE Int. Conf. Robot. Automat.*, San Francisco, CA, April 2000, pp. 1068–1075.

[14] J. Ponce and B. Faverjon, "On computing three finger force-closure grasp of polygonal objects," *IEEE Trans. Robot. Automat.*, vol. 11, no. 6, pp. 868–881, 1995.

[15] R. Kurazume and S. Hirose, "Study on cooperative positioning system - optimum moving strategies for $cpsiii$," in *Proc. IEEE Int. Conf. Robot. Automat.*, Leuven, Belgium, May 1998, pp. 2896–2903.

[16] R. Fierro, A. Das, V. Kumar, and J. P. Ostrowski, "Hybrid control of formation of robots," To appear in IEEE Int. Conf. Robot. Automat., ICRA01, May 2001.

[17] R. Alur, A. Das, J. Esposito, R. Fierro, Y. Hur, G. Grudic, V. Kumar, I. Lee, J. P. Ostrowski, G. Pappas, J. Southall, J. Spletzer, and C. J. Taylor, "A framework and architecture for multirobot coordination," in *Proc. ISER00, Seventh International Symposium on Experimental Robotics*, Honolulu, Hawaii, Dec. 2000.

[18] A. Nadas, "Least squares and maximum likelihood estimation of rigid motion," Tech. Rep., IBM, 1978.

[19] J. Desai, J. P. Ostrowski, and V. Kumar, "Controlling formations of multiple mobile robots," in *Proc. IEEE Int. Conf. Robot. Automat.*, Leuven, Belgium, May 1998, pp. 2864–2869.

[20] A. Isidori, *Nonlinear Control Systems*, Springer-Verlag, London, 3rd edition, 1995.

[21] H. Khalil, *Nonlinear Systems*, Prentice Hall, Upper Sadle River, NJ, 2nd edition, 1996.

[22] S. Baker and S. Nayar, "A theory of catadoptric image formation," in *International COnference on Computer Vision*, Bombay, India, Jan 1998, pp. 35–42.

[23] A. Das, R. Fierro, V. Kumar, J. Southall, J. Spletzer, and C. J. Taylor, "Real-time vision based control of a non-holonomic mobile robot," To appear in IEEE Int. Conf. Robot. Automat., ICRA01, May 2001.